Research Square

Preprints are preliminary reports that have not undergone peer review.
They should not be considered conclusive, used to inform clinical practice,
or referenced by the media as validated information.

Acute psychosocial stress and exhaustive exercise converge on a granulocyte-derived cfDNA signature

Dirk Moser

dirk.moser@rub.de

Ruhr University Bochum / Genetic Psychology https://orcid.org/0000-0002-7021-1204

Fabian Berg

Sven Berres

Ruhr University Bochum / Genetic Psychology https://orcid.org/0000-0002-9241-9137

Kerstin Becker

Petra Platen

Markus de Marees

Robert Kumsta

University of Luxemburg https://orcid.org/0000-0001-6006-6958

Julian Uszkoreit

Ruhr University Bochum https://orcid.org/0000-0001-7522-4007

Article

Keywords:

Posted Date: November 19th, 2026

DOI: https://doi.org/10.21203/rs.3.rs-11289856/v1

License: This work is licensed under a Creative Commons Attribution 4.0 International License.
Read Full License

Additional Declarations: The authors have declared there is **NO** conflict of interest to disclose

Abstract

Circulating cell-free DNA (cfDNA) increases rapidly after acute psychosocial and physical stress, but its cellular origins remain incompletely understood. We investigated whether stress-induced cfDNA originates from tissues directly engaged by each stressor or reflects a shared cellular response. Six healthy young men completed the Trier Social Stress Test (TSST), an exhaustive graded exercise test (GXT), and the Cold Pressor Test (CPT) in a within-subject design. Plasma was collected before and 2, 15, and 45 min after each stressor. CfDNA concentrations were quantified by droplet digital PCR, and genome-wide methylation profiling using enzymatic methyl-seq was used to infer cellular origins. All three paradigms elicited distinct neuroendocrine responses. Both the TSST and GXT increased circulating cfDNA, with granulocytes representing a major contributing cell type, whereas the CPT induced no comparable cfDNA response. The increase was substantially larger following GXT than TSST. Baseline cfDNA was predominantly hematopoietic and highly consistent across participants and experimental days. Neither neuronal nor skeletal muscle-derived cfDNA showed substantial stress-induced increases. Two complementary deconvolution approaches consistently reproduced the granulocyte-associated signature. Genome-wide cfDNA profiles were conserved across stressors, but fragments were non-randomly enriched in genic, CpG-rich, and neutrophil chromatin regions. Acute psychosocial stress and exhaustive exercise therefore converge on a shared cfDNA response with a major granulocyte contribution. Previous evidence suggests that this signal may predominantly originate from neutrophils and could involve NET-associated DNA release; however, the present data do not directly resolve granulocyte subtypes or the underlying release mechanism.

Introduction

Cell-free DNA (cfDNA) consists of short DNA fragments released into the circulation through cell death and regulated cellular release mechanisms. Although present at relatively low concentrations under physiological conditions, plasma cfDNA concentrations can change within minutes in response to acute perturbations, making it a sensitive marker of cellular and tissue responses. Beyond its established clinical applications in non-invasive prenatal testing, transplantation monitoring, and cancer diagnostics [1-3], cfDNA has increasingly attracted attention as a biomarker of acute physiological stress [4]. Both intense physical exercise and acute psychosocial stress have been shown to rapidly increase circulating cfDNA concentrations, although the response to exhaustive exercise is typically considerably larger than that observed after psychosocial stress [5-8]. What remains less clear is whether these quantitatively different responses arise from the same cellular sources and reflect common or stressor-specific mechanisms of cfDNA release.

Determining the cellular origin of circulating cfDNA is essential for understanding its biological significance. In healthy individuals, most plasma cfDNA is derived from hematopoietic cells, although estimates of individual cell-type contributions vary depending on the analytical approach and reference populations used. Genome-wide DNA methylation and fragmentomic studies have identified granulocytes, lymphocytes, monocytes, erythroid progenitors, and megakaryocytes as major contributors

to the basal cfDNA pool [9-18]. More recent methylation-based analyses have further indicated that neutrophils constitute a particularly large fraction of leukocyte-derived cfDNA [12-14]. Importantly, the cellular composition of cfDNA is not static but changes in response to physiological challenges, providing an opportunity to use cfDNA not only as a quantitative biomarker but also as a molecular readout of the cells responding to a particular stimulus.

This has been demonstrated most clearly for physical exercise. Acute strenuous exercise produces a rapid and pronounced increase in circulating cfDNA, and recent cell-of-origin studies consistently indicate that this additional cfDNA originates predominantly from mature neutrophils [19-21]. Methylation-based analyses have attributed the majority of exercise-induced cfDNA to leukocytes, with neutrophils accounting for the dominant proportion, while genome-wide approaches have additionally identified smaller contributions from other innate immune cell populations [19-21]. These observations suggest that the substantial increase in cfDNA during exercise reflects an acute and highly dynamic response of the innate immune system rather than nonspecific cellular damage alone. However, it remains unclear whether neutrophil-derived cfDNA release represents a general feature of acute stress or is preferentially associated with the complex physiological demands of strenuous exercise.

This distinction is particularly relevant because different acute stress paradigms engage overlapping but clearly distinct physiological pathways. Psychosocial stress, as induced by the Trier Social Stress Test (TSST, [22]), activates the hypothalamic-pituitary-adrenal (HPA) axis together with sympathetic pathways and reliably induces cortisol responses [22]. Exhaustive physical exercise combines sympathetic and HPA-axis activation with major cardiovascular, metabolic, mechanical, and immune changes [23]. In contrast, the Cold Pressor Test (CPT [24, 25]) provides a strong nociceptive and predominantly sympatho-adrenergic challenge, characterized by rapid cardiovascular and catecholaminergic responses but comparatively limited activation of several physiological processes associated with exhaustive exercise [24-26]. Comparing these stressors may therefore help distinguish whether acute cfDNA release is a general consequence of sympathetic activation or requires additional stressor-specific signals.

Previous work from us and other groups demonstrated that both psychosocial stress and exhaustive exercise induce rapid increases in circulating nuclear cfDNA, while physical exercise produces substantially larger responses [6-8, 27]. We additionally observed stressor-dependent differences in cfDNA fragmentation and locus-specific DNA methylation, suggesting that psychosocial and physical stress may differ not only in the magnitude of cfDNA release but potentially also in its cellular origin [7]. At the time, however, the cellular composition of stress-induced cfDNA could not be resolved. While recent studies have since established neutrophils as the predominant source of exercise-induced cfDNA [19-21], the cellular origin of cfDNA released during acute psychosocial stress has remained largely unknown. Moreover, whether a predominantly sympatho-adrenergic stressor in the absence of exhaustive physical activity is sufficient to elicit a comparable cfDNA response has not been systematically addressed (Table S1).

DNA methylation provides a powerful means of resolving this question because methylation patterns are highly cell-type specific and remain preserved in cfDNA fragments after their release into the circulation [9, 11, 12, 14, 28]. For example, previous studies reported that physical exercise can induce dynamic and tissue-specific epigenetic changes, including alterations in skeletal muscle DNA methylation [29]. Genome-wide methylation-based deconvolution compares cfDNA methylation profiles with reference methylomes from purified cell populations and thereby estimates the relative contribution of individual cell types to the circulating cfDNA pool [9, 11, 12, 14]. Advances in high-resolution methylation reference atlases have substantially increased the ability to distinguish closely related hematopoietic populations and thus provide an opportunity to characterize acute changes in cfDNA composition with greater cellular resolution.

Here, we used genome-wide cfDNA methylation profiling to directly compare three complementary acute stress paradigms: the TSST as a psychosocial stressor [22], a graded exercise test to volitional exhaustion (GXT) as an intense physical stressor [7, 30], and the CPT as a predominantly sympatho-adrenergic challenge [24, 25]. By combining serial cfDNA measurements with methylation-based cell-of-origin deconvolution, we examined whether these stressors differ not only quantitatively in cfDNA dynamics, but also qualitatively regarding their cellular origin, and whether sympathetic activation alone is sufficient to induce a comparable cfDNA response.

Materials and Methods

Participants and study design

Six healthy male sport science students (20–23 years; mean age 21.6 ± 1.2 years; BMI 23.98 ± 1.9 kg/m²) participated in this exploratory within-subject repeated-measures study. Each participant underwent three experimentally induced stress tests on separate experimental days: psychosocial stress induced by the TSST, physical stress induced by GXT, and nociceptive stress induced by CPT. Experimental sessions were separated by at least one week and were performed in the same order (TSST → GXT → CPT). Because of the exploratory character and limited sample size of this pilot study, stressor order was not randomized.

Participants were recruited from the sport science program at Ruhr University Bochum. Inclusion criteria comprised good general health and medical clearance for participation in practical sports courses. Exclusion criteria included current or previous mental disorders, acute or chronic physical illness, current medication use, and recreational drug use. Participants were instructed to refrain from vigorous physical exercise for at least 4 h and from large meals for at least 1 h before testing. To minimize circadian variation in endocrine stress responses, all experimental sessions were conducted between 14:00 and 16:00 h. All participants provided written informed consent. The study was approved by the Ethics Committee of the Faculty of Psychology at Ruhr University Bochum (reference no. 934/2024) and conducted in accordance with the Declaration of Helsinki.

Experimental procedure

Upon arrival at the laboratory, participants completed the Physical Activity Readiness Questionnaire (PAR-Q), which was reviewed by a sports physician, and subsequently remained seated in a quiet room before stress exposure. An indwelling venous catheter was inserted into an antebrachial or cubital vein 45 min before stress induction to enable repeated blood collection while minimizing procedural stress. Blood samples were obtained at −2 min relative to stressor onset and at +2, +15, and +45 min thereafter. Heart rate and blood pressure were monitored continuously throughout the protocol. Subjective emotional responses were assessed at the corresponding time points using the Social Emotional Response Scale (SERS), covering arousal, self-directed emotions, and anxiety.

Stress paradigms

The TSST was performed according to the established standardized protocol[22] and comprised a preparation period followed by a free-speech task and an unanticipated mental arithmetic task performed in front of an evaluative panel and a video camera.

Physical stress was induced using an exhaustive graded treadmill exercise test (GXT). Participants first completed a 5-min warm-up walk at 1.0 m/s and a 15% incline. Thereafter, treadmill speed increased by 0.2 m/s every 30 s until participants reached subjective exhaustion, at which point the treadmill was stopped. Mean exercise duration was 9 min 56 s ± 58 s.

For the CPT, participants immersed their non-dominant hand up to the wrist in ice-cold water maintained at 1–3 °C for up to 3 min. All participants completed the full 3-min exposure.

Plasma preparation and hormone measurements

Whole blood was collected into 9-mL EDTA tubes and immediately centrifuged at 1,600 × g for 10 min at 4 °C. The plasma fraction was transferred to fresh tubes and centrifuged again at 16,000 × g for 10 min at 4 °C to remove residual cells and cellular debris. Plasma was aliquoted for hormone analyses, cfDNA quantification, and cfDNA isolation and stored at −80 °C until further processing.

Plasma cortisol concentrations were measured using a commercial Chemiluminescence immunoassay (CLIA; Tecan/IBL, Hamburg; Germany). Adrenaline and noradrenaline concentrations were quantified by high-performance liquid chromatography at the Laboratory for Stress Monitoring (LSM, Göttingen; Germany).

Plasma cfDNA quantification by droplet digital PCR

Building on our previous work establishing ddPCR-based approaches for sensitive and reproducible absolute DNA quantification [31], plasma cfDNA concentrations were quantified using a multicopy droplet digital PCR (ddPCR) assay targeting a conserved 110-bp sequence within the LINE-1 L1PA2 subfamily (Table S2). The assay was analytically optimized using serial dilutions to establish the linear

quantification range, exclude relevant plasma-associated inhibition, and optimize separation of positive and negative droplet populations. Based on these experiments, plasma samples were diluted 1:20 for subsequent measurements. Reactions yielding fewer than 12,500 accepted droplets were excluded from quantitative analysis.

Adapted from our previously described qPCR assay [8], reactions were performed in a final volume of 20 µL using ddPCR Supermix for Probes, 900 nM of each L1PA2 primer, 300 nM FAM-labelled hydrolysis probe, and 1.5 µL of 1:20 diluted plasma. Samples were analyzed in technical duplicates using a QX600 Droplet Digital PCR System (Bio-Rad Laboratories, Hercules; USA). Droplet fluorescence thresholds were defined per run based on the corresponding no-template controls and applied consistently across all samples and technical replicates within that run. Concentrations were calculated using Poisson-based quantification.

The genomic abundance of the targeted L1PA2 sequence was assessed in silico, and the resulting copy numbers were converted to plasma cfDNA concentrations by accounting for plasma dilution, reaction volume, the predicted number of amplifiable L1PA2 loci per haploid genome, and a DNA content of ~3.3 pg per haploid genome.

cfDNA isolation and methylation sequencing

For genome-wide methylation analyses, cfDNA was isolated from 3 mL plasma using the QIAamp Circulating Nucleic Acid Kit (Qiagen, Hilden; Germany). CfDNA concentration, fragment-size distribution, and integrity were assessed using a Fragment Analyzer equipped with the DNF-477 High Sensitivity NGS Fragment Analysis Kit (Agilent Technologies, Santa Clara; USA).

Libraries were generated from 10 ng cfDNA using the NEBNext Enzymatic Methyl-seq kit (EM-seq; New England Biolabs, Ipswich; USA). This enzymatic conversion strategy was selected to minimize additional DNA degradation and preserve library complexity in the highly fragmented cfDNA samples. Libraries were prepared for all available samples corresponding to six participants, three stress paradigms, and four sampling time points. Sequencing was performed on an Illumina NovaSeq 6000 platform using 2 × 100-bp paired-end sequencing (Illumina, San Diego; USA), targeting approximately 110 million read pairs per sample.

Bioinformatic processing and cell-of-origin deconvolution

Raw paired-end sequencing reads were processed using the nf-core/methylseq pipeline with the EM-seq option enabled. Reads were aligned to the GRCh38 human reference genome (Ensembl release 113), and methylation calls were generated using Bismark [32].

Cell-of-origin contributions to circulating cfDNA were estimated using two complementary reference-based deconvolution approaches. First, fragment-level deconvolution was performed using the UXM framework [12], which exploits co-methylation patterns across multiple CpGs within individual cfDNA

fragments. Second, non-negative least squares (NNLS) deconvolution was performed using cell-type reference methylomes derived from the Moss methylation atlas [12, 14]. Together, these approaches provided complementary estimates of cell-type-specific cfDNA contributions based on site-level and fragment-level methylation patterns.

Genomic distribution and annotation enrichment of cfDNA

Genome-wide coverage profiling

Genome-wide cfDNA distribution was assessed in 72 paired-end EM-seq libraries from six participants exposed to three acute stress paradigms (TSST, GXT, and CPT) at four sampling time points. Reads were processed using nf-core/methylseq v2 against GRCh38 (Ensembl 113). Read coverage was quantified in non-overlapping 100-kb genomic bins using samtools bedcov [33]. For each sample, mean coverage per bin was normalized to the genome-wide mean coverage across autosomal, non-blacklisted regions, yielding a fold-change over uniform genomic representation (FC), with FC = 1 indicating average genome-wide coverage.

Regions overlapping the ENCODE hg38 blacklist were excluded. In addition, chr9:130.0–138.3 Mb was removed after quality-control analyses identified recurrent extreme coverage values associated with low-complexity and highly duplicated libraries, consistent with non-unique read mapping in this repeat-rich region. Sex chromosomes were excluded to avoid sex-dependent differences in genomic representation. Normalized coverage values were averaged across the four time points within each stress condition and visualized across chromosomes 1-22.

Genomic annotation enrichment.

To determine whether cfDNA fragments were non-randomly distributed across genomic features, 700 properly paired fragments were reservoir-sampled from each library, resulting in 50,400 fragments. Fragments were restricted to canonical chromosomes and insert sizes of 50–1,000 bp. Enrichment was assessed using regioneR permutation testing with 500 permutations [34]. Fragment positions were randomized across the canonical hg38 genome and observed overlaps with genomic annotations were compared with overlaps expected under random placement.

Annotations comprised promoters, 5'UTRs, exons, introns, 3'UTRs, CpG islands, intergenic regions, major RepeatMasker classes, and ENCODE ChIP-seq regions for H3K27ac, H3K27me3, and H3K9me3 in primary human neutrophils. Enrichment was expressed as Z-scores and as fold change relative to the mean number of overlaps obtained from randomized datasets. P-values were adjusted across annotation tests using the Benjamini–Hochberg false-discovery rate procedure.

Statistical analysis

Statistical analyses were performed in RStudio (version 2026.09.0+174 [35, 36]). Endocrine markers, cfDNA concentrations, and methylation-based cell-of-origin estimates were analyzed using two-way repeated-measures ANOVA, with stress paradigm and time point as within-subject factors. Given the exploratory

nature of this study and the limited sample size, estimated cell types were grouped according to the categories presented in the original publications. Neuronal and skeletal muscle-derived cfDNA were considered separately because of their specific relevance to the present study and were therefore not included in the “Other” category in the UXM framework. Only cell types showing a significant stress paradigm × time point interaction were followed up with paired t-tests comparing each post-stressor time point with the corresponding baseline. P-values from follow-up comparisons were adjusted for multiple testing using the Benjamini–Hochberg false-discovery rate procedure. The assumption of normality was assessed using Shapiro–Wilk tests. If necessary, degrees of freedom were adjusted when the assumption of sphericity was violated. Two-sided p-values < .05 were considered statistically significant. Effect sizes are reported as partial η^2 for ANOVA effects and Cohen’s d with 95% confidence intervals for paired comparisons. Mean values are reported as mean ± SD. No outliers were removed.

Results

Overall, Shapiro–Wilk tests indicated no substantial deviations from normality. Therefore, the statistical analyses were performed on the data as presented. All three stress tests elicited distinct neuroendocrine response profiles (Figure 2B-D). The TSST showed significant elevations in plasma cortisol at +2 min ($t(5) = -3.71$, $p = .021$, $d = -1.52$ [-4.35, -0.92]) and +15 min after the stressor ($t(5) = -3.94$, $p = .021$, $d = -1.61$ [-5.11, -1.14]). Similarly, noradrenaline concentrations peaked directly after the TSST ($t(5) = -10.8$, $p < .001$, $d = -4.41$ [-14.2, -3.61]) and remained significantly elevated after +15 min ($t(5) = -6.32$, $p < .01$, $d = -2.58$ [-7.35, -2.11]). While cortisol concentration was increased by a maximum fold of 1.56 and noradrenaline levels by a fold of 1.9 after the TSST, GXT elicited an even more pronounced response. Plasma cortisol was significantly increased at +15 min ($t(5) = -5.56$, $p < .01$, $d = -2.27$ [-7.09, -1.52]) and +45 min ($t(5) = -4.93$, $p < .01$, $d = -2.01$ [-17.6, -1.41]), whereas the noradrenaline concentration was significantly elevated at +2 min ($t(5) = -3.25$, $p = .035$, $d = -1.33$ [-5.26, -0.97]) and +15 min ($t(5) = -3.22$, $p = .035$, $d = -1.32$ [-3.03, -0.94]) after GXT. In contrast to the TSST, however, GXT resulted in a maximum 2.11-fold increase of cortisol levels and an 11.34-fold increase of the noradrenaline concentration. On the other hand, plasma cortisol and noradrenaline were elevated at maximum by a fold of 1.51 after the CPT, which was at a trend level but not statistically significant following adjustment for multiple testing. Furthermore, at +2 min, no stressor showed significant alterations in the adrenaline concentration. Solely GXT induced a significant increase in adrenaline levels at +15 min ($t(4) = -6.18$, $p = .01$, $d = -2.76$ [-8.38, -1.99]) and +45 min ($t(4) = -3.43$, $p = .04$, $d = -1.53$ [-3.83, -1.07]).

Taken together, the TSST predominantly induced a pronounced cortisol response with a comparatively moderate catecholamine response, whereas GXT elicited marked increases in both catecholamines and cortisol. The CPT showed a distinct but statistically less robust neuroendocrine response.

Baseline plasma cfDNA concentrations, assessed in all six participants on three separate experimental days approximately one week apart, averaged 4.52 ± 1.41 ng/mL. Consistent with the stressor-specific response patterns, cfDNA increased 2.47-fold following the TSST and 6.54-fold following GXT, whereas CPT did not induce a consistent cfDNA increase within the investigated time window. (Figure 2A).

However, only cfDNA levels after GXT reached statistical significance at +2 min ($t(5) = -5.62$, $p < .01$, $d = -2.29$ [-44.3, -1.54]), + 15 min ($t(5) = -6.91$, $p < .01$, $d = -2.82$ [-6.65, -1.94]) and +45 min ($t(5) = -5.20$, $p < .01$, $d = -2.12$ [-7.62, -1.27]), while cfDNA levels at +2 min and +15 min after the TSST remained at trend level ($p = .06$).

Genome-wide DNA methylation-based cell-of-origin analyses demonstrated highly reproducible cfDNA profiles across participants and study days under resting conditions, indicating a high degree of within-participant reproducibility and similar baseline profiles across participants (Figure 3A-H). Baseline samples exhibited a remarkably consistent cellular composition across all three experimental sessions. Both deconvolution approaches indicated that circulating cfDNA originated predominantly from hematopoietic cells, with granulocytes representing the largest identifiable cellular fraction, whereas contributions from non-hematopoietic tissues were consistently low (Figure 3A-B).

Although the overall composition of circulating cfDNA remained largely stable following acute stress exposure, stressor-dependent alterations in cell-of-origin became evident. Repeated measures ANOVAs revealed significant stress ´ time interactions for granulocytes ($F(6, 30) = 5.00$, $p < .01$, $h^2_p = .50$), megakaryocytes ($F(6, 30) = 3.43$, $p = .037$, $h^2_p = .41$) and vascular endothelial cells ($F(6, 30) = 3.48$, $p = .037$, $h^2_p = .41$) in the UXM framework. In addition, the NNLS framework identified significant interaction effects for granulocytes ($F(6, 30) = 9.52$, $p < .001$, $h^2_p = .66$) and erythrocyte progenitor cells ($F(6, 30) = 3.54$, $p = .027$, $h^2_p = .41$). Follow-up analysis showed that both GXT and TSST were associated with an increased contribution of granulocyte-derived cfDNA. Notably, the magnitude of this response differed considerably. Precisely, the granulocyte fraction was elevated significantly at +2 min ($t(5) = -3.47$, $p = .018$, $d = -1.42$ [-7.91, -1.20]), +15 min ($t(5) = -6.72$, $p < .01$, $d = -2.74$ [-11.7, -2.22]) and +45 min ($t(5) = -10.26$, $p < .001$, $d = -4.19$ [-24.5, -3.40]) after GXT in the UXM framework and at +2 min ($t(5) = -7.80$, $p < .01$, $d = -3.18$ [-7.82, -2.33]), +15 min ($t(5) = -6.42$, $p < .01$, $d = -2.62$ [-5.49, -2.22]) and +45 min ($t(5) = -5.51$, $p < .01$, $d = -2.25$ [-5.66, -1.49]) in the NNLS framework (Figure 3C-D). This increase was accompanied by a significant decrease in megakaryocyte and vascular endothelium levels utilizing UXM and erythrocyte progenitors using NNLS (ps < .05). For the TSST, the percentage of granulocytes was significantly increased at +15 min ($t(5) = -3.66$, $p = .044$, $d = -1.49$ [-4.78, -1.24]) in the UXM framework and at +2 min ($t(5) = -2.92$, $p = .05$, $d = -1.19$ [-3.98, -0.41]) and +15 min ($t(5) = -2.92$, $p = .05$, $d = -1.19$ [-3.33, -0.57]) when estimating with NNLS (Figure 3E-F). As increases in the granulocyte fraction following TSST were at maximum 11% and 14%, respectively for UXM and NNLS, no significant decreases were revealed. In contrast, the portion of granulocytes increased up to 29% and 38% following GXT, respectively for UXM and NNLS. Hence, the TSST induced a moderate increase in granulocyte-derived cfDNA, whereas GXT resulted in a pronounced expansion of the granulocyte fraction, accounting for most of the observed increase in circulating cfDNA. In contrast, the CPT elicited only minor changes in cfDNA composition (Figure 3G-H). Across all stress conditions, contributions from neuronal and skeletal muscle-derived cfDNA remained low and showed no substantial stress-induced alterations.

Despite marked differences in the physiological characteristics of the three stress tests, GXT and TSST shared a common cell-of-origin signature characterized by an increased contribution of granulocyte-derived cfDNA. In contrast, the relative contributions of most other cell populations remained largely unchanged or decreased throughout the experimental period. Thus, when cfDNA increases in response to acute stress, the response appears to be predominantly attributable to granulocyte-derived cfDNA rather than to widespread shifts in tissue-of-origin composition.

Comparison of two complementary deconvolution approaches, UXM and NNLS, demonstrated a high degree of agreement across baseline and stress conditions. Both approaches consistently identified hematopoietic cells as the predominant cellular source of circulating cfDNA and reproduced the stress-associated increase in granulocyte-derived cfDNA observed after GXT and TSST. This concordance across conceptually complementary but distinct deconvolution frameworks strengthens confidence in the robustness of the observed granulocyte-dominated cfDNA signature but does not by itself resolve the contributing granulocyte subtype.

Genome-wide cfDNA representation was highly structured and remarkably conserved across stress paradigms (Figure 4A). Despite pronounced differences in total cfDNA concentrations between TSST, GXT, and CPT, broad chromosomal coverage profiles remained highly similar, with no apparent large-scale condition-specific shifts. This suggests that acute stress primarily altered cfDNA abundance rather than its overall genomic representation.

At the same time, permutation analysis demonstrated that cfDNA fragments were distributed in a strongly non-random manner across genomic annotations (Figure 4B). Genic and CpG-rich regions were significantly enriched, whereas intergenic regions were markedly depleted. Among repeat elements, SINEs and LTRs were enriched, while LINEs, satellite repeats, simple repeats, and low-complexity regions were depleted, with satellite repeats showing the strongest depletion. cfDNA fragments were also significantly enriched across the examined chromatin states defined in primary human neutrophils, including both active (H3K27ac) and repressive (H3K27me3, H3K9me3) domains. Although the overall chromosomal distribution of cfDNA remained largely conserved across stress conditions, its genomic representation was therefore structured at the level of functional annotations and chromatin context. The overlap with neutrophil reference chromatin was compatible with, but did not independently prove, a neutrophil contribution to the granulocytic signal.

Discussion

The present study provides a genome-wide methylation-based comparison of cfDNA cell-of-origin profiles across three fundamentally distinct acute stress tests. Despite substantial differences in the physiological characteristics of psychosocial stress, exhaustive exercise, and sympathetic activation, GXT and TSST converged on a similar cellular signature characterized by an increased contribution of granulocyte-derived cfDNA. Together, these findings indicate a shared granulocytic response rather than tissue-specific DNA release from tissues primarily engaged by the respective stressors.

A key finding of the present study is that the increases in circulating cfDNA following acute psychosocial stress and exhaustive exercise were not accompanied by detectable increases in cfDNA derived from tissues that might intuitively be expected to contribute to each response. Psychosocial stress strongly engages central neuroendocrine processes, whereas exhaustive exercise places substantial physiological demands on skeletal muscle. Given the extensive metabolic, inflammatory, structural, and epigenetic responses of skeletal muscle to acute exercise [37], a contribution of skeletal muscle-derived cfDNA therefore appeared biologically plausible. Nevertheless, neither neuronal nor skeletal muscle-derived cfDNA showed substantial stress-induced increases. Instead, genome-wide methylation-based cell-of-origin analyses consistently identified granulocytes as the predominant source of stress-induced cfDNA. Thus, the tissue subjected to the greatest physiological demand is not necessarily the tissue contributing most prominently to circulating cfDNA. This observation has important implications for the interpretation of circulating cfDNA during acute physiological challenges. Cell-free DNA has frequently been considered a marker of tissue damage or increased cellular turnover within the organ primarily affected by a disease or physiological stimulus [11, 38]. Our findings suggest that this concept cannot simply be transferred to acute stress. Instead, distinct stressors appear to converge on a common downstream cfDNA signature characterized by a predominant granulocyte contribution. Acute stress-associated cfDNA may therefore primarily reflect systemic innate immune processes rather than cfDNA release from the tissues most directly engaged by each stressor. In the case of exhaustive exercise, our findings argue against skeletal muscle microinjury as a major source of the circulating cfDNA increase.

Although all three stress tests elicited distinct responses involving activation of sympathetic and/or hypothalamic-pituitary-adrenal pathways, only psychosocial stress was associated with a moderate cfDNA increase, whereas exhaustive exercise induced a pronounced increase in circulating cfDNA. Thus, activation of classical neuroendocrine stress pathways alone appears insufficient to explain acute cfDNA release [39]. Additional downstream physiological processes are likely required before measurable cfDNA elevations occur. The predominance of granulocyte-derived cfDNA after GXT and TSST points to granulocyte-associated processes as a common downstream component. Previous exercise studies identified mature neutrophils as a principal source and proposed neutrophil activation in response to muscle damage as a possible mechanism [19]. Our granulocyte-level finding is compatible with this interpretation but does not independently establish neutrophil origin. Moreover, the granulocyte-derived cfDNA increase after psychosocial stress, which does not involve exercise-induced muscle damage, suggests that muscle damage is not a prerequisite and points to a broader stress-responsive mechanism.

We hypothesize that neutrophils account for a substantial part of the granulocyte-derived cfDNA response. This interpretation is supported by prior exercise-specific cell-of-origin studies identifying mature neutrophils and by evidence that acute psychological and physical stress can induce rapid neutrophil mobilization through catecholamine-mediated demargination and glucocorticoid-dependent redistribution [19-21, 40]. Exhaustive exercise has also been associated with transient sterile inflammation, neutrophil activation, and formation of neutrophil extracellular traps (NETs), providing a plausible route

for extracellular DNA release [41-43]. Nevertheless, the present study neither resolves granulocyte subtypes nor includes NET-specific markers. Neutrophil involvement and NET-associated release therefore remain mechanistic hypotheses rather than direct findings of this study.

Importantly, the pronounced granulocyte-derived cfDNA response observed after exercise should be interpreted in the context of the specific exercise test employed. GXT is a widely used approach for assessing exercise capacity and the integrated physiological response to progressively increasing exercise [44], with maximal protocols imposing substantial physiological stress as participants are exercised to volitional exhaustion. Consequently, the observed cfDNA response is unlikely to represent the biology of health-promoting physical activity but rather the consequences of maximal physiological strain. This distinction is particularly relevant because regular moderate-to-vigorous exercise is generally associated with anti-inflammatory and long-term health-protective adaptations [45], whereas exhaustive exercise may transiently induce inflammatory responses and immune activation [46].

Future studies should therefore directly compare maximal exercise with standardized submaximal exercise protocols representing health-promoting exercise intensities. Such experiments will help determine whether the granulocyte-derived cfDNA response is a biomarker of extreme physiological stress or whether distinct cell-of-origin profiles emerge during exercise that induces beneficial physiological adaptations. From this perspective, replacing the CPT with a controlled submaximal exercise condition may provide considerably greater biological insight into the relationship between physical activity, granulocyte activation, and cfDNA release.

An additional noteworthy finding was the remarkable stability of baseline cfDNA composition. Genome-wide methylation profiles were highly reproducible across participants and repeated study days despite being collected on separate experimental occasions. This high reproducibility across repeated baseline measurements supports the robustness of methylation-based cell-of-origin analyses and provides confidence that the stress-induced alterations observed here reflect genuine biological responses rather than random variation or technical noise.

Importantly, the principal findings were reproduced by two conceptually distinct deconvolution frameworks. Despite relying on different analytical approaches, both NNLS and UXM consistently identified granulocytes as the predominant source of stress-induced cfDNA. This concordance strengthens confidence that the observed granulocyte signature reflects a genuine biological phenomenon rather than an artefact of a particular computational method.

Consistent with the methylation-based deconvolution results, cfDNA fragments were enriched within chromatin domains defined in primary human neutrophils. This provides complementary evidence that the granulocytic signal is compatible with a neutrophil contribution, although overlap with a reference chromatin annotation does not independently establish cellular identity. Genome-wide coverage profiles were remarkably similar across TSST, GXT, and CPT despite substantial differences in total cfDNA concentrations, suggesting that acute stress predominantly alters cfDNA quantity rather than broad

genomic composition. At the same time, cfDNA fragments were non-randomly distributed across the genome, with enrichment in genic and CpG-rich regions and depletion of intergenic and satellite-rich regions. This pattern indicates that cfDNA generation and/or persistence is shaped by genomic and chromatin organization [11].

Notably, the observed enrichment extended across both transcriptionally active and repressive neutrophil chromatin states, suggesting that the signal was not restricted to a single functional chromatin compartment. This observation is compatible with the hypothesis that neutrophils contribute substantially to the granulocyte-derived cfDNA signal, but it should not be interpreted as an independent cell-of-origin assignment. Enrichment was not restricted to active chromatin, indicating that cfDNA release cannot simply be explained by preferential liberation of transcriptionally active genomic regions. Together, these findings support the concept that stress-induced cfDNA release is a structured biological process rather than a nonspecific consequence of generalized cell damage [11, 15, 16].

Several limitations should be acknowledged. As a pilot study, the present investigation included only six healthy young men and therefore, some potential effects did not reach the level of statistical significance and require replication in larger and more diverse populations. In addition, stressor order was not randomized, and potential order or habituation effects cannot be excluded. Critically, the deconvolution analyses consistently supported a granulocyte origin but did not provide sufficiently robust resolution to assign the signal to a specific granulocyte subtype. The proposed predominance of neutrophils is therefore based on biological plausibility and prior exercise studies rather than direct subtype identification in the present dataset. Finally, methylation-based deconvolution cannot distinguish among NETosis, apoptosis, necrosis, and other forms of extracellular DNA release. Direct quantification of neutrophil-specific methylation markers together with NET-associated proteins and cell-death markers will be required to test the proposed mechanism.

In conclusion, our findings challenge the assumption that acute stress-induced cfDNA primarily reflects DNA release from the tissue most strongly affected by the stressor. Instead, psychosocial stress and exhaustive exercise converged on a shared granulocyte-derived and genomically structured cfDNA signature. Prior evidence makes neutrophils, potentially undergoing NET-associated DNA release, a compelling candidate source; however, this mechanistic interpretation remains to be tested directly.

Declarations

ACKNOWLEDGEMENTS

The authors thank Alicia Limberg for preparing the study and Kim Walusiacki for her expert technical assistance. We further acknowledge support by the Open Access Publication Funds of Ruhr University Bochum.

AUTHOR CONTRIBUTIONS

DAM and FB designed the study. DAM, FB, and MdM performed the experiments. SB and JU conducted the bioinformatic analyses, including deconvolution and genomic alignment, with support from FB. FB, SB, PP, MdM, KB, RK, JU, and DAM evaluated the data and interpreted the experimental results. DAM wrote the initial draft of the manuscript, and all authors reviewed and edited the manuscript.

ETHICS DECLARATION

The study was conducted in accordance with the Declaration of Helsinki and approved by the Ethics Committee of the Faculty of Psychology at Ruhr University Bochum (reference no. 934/2024). Written informed consent was obtained from all participants.

COMPETING INTERESTS

The authors declare no competing interests.

References

1. Bettegowda C, Sausen M, Leary RJ, Kinde I, Wang Y, Agrawal N, Bartlett BR, Wang H, Luber B, Alani RM, Antonarakis ES, Azad NS, Bardelli A, Brem H, Cameron JL, Lee CC, Fecher LA, Gallia GL, Gibbs P, Le D, Giuntoli RL, Goggins M, Hogarty MD, Holdhoff M, Hong SM, Jiao Y, Juhl HH, Kim JJ, Siravegna G, Laheru DA, Lauricella C, Lim M, Lipson EJ, Marie SK, Netto GJ, Oliner KS, Olivi A, Olsson L, Riggins GJ, Sartore-Bianchi A, Schmidt K, Shih I M, Oba-Shinjo SM, Siena S, Theodorescu D, Tie J, Harkins TT, Veronese S, Wang TL, Weingart JD, Wolfgang CL, Wood LD, Xing D, Hruban RH, Wu J, Allen PJ, Schmidt CM, Choti MA, Velculescu VE, Kinzler KW, Vogelstein B, Papadopoulos N, Diaz LA, Jr. Detection of circulating tumor DNA in early- and late-stage human malignancies. *Sci Transl Med* 2014; 6(224): 224ra224.
2. Lo YM, Corbetta N, Chamberlain PF, Rai V, Sargent IL, Redman CW, Wainscoat JS. Presence of fetal DNA in maternal plasma and serum. *Lancet* 1997; 350(9076): 485–487.
3. Snyder TM, Khush KK, Valantine HA, Quake SR. Universal noninvasive detection of solid organ transplant rejection. *Proc Natl Acad Sci U S A* 2011; 108(15): 6229–6234.
4. Trumpff C, Michelson J, Lagranha CJ, Taleon V, Karan KR, Sturm G, Lindqvist D, Fernstrom J, Moser D, Kaufman BA, Picard M. Stress and circulating cell-free mitochondrial DNA: A systematic review of human studies, physiological considerations, and technical recommendations. *Mitochondrion* 2021; 59: 225–245.
5. Breitbach S, Tug S, Simon P. Circulating cell-free DNA: an up-coming molecular marker in exercise physiology. *Sports medicine* 2012; 42(7): 565–586.
6. Herhaus B, Neuberger E, Juskeviciute E, Simon P, Petrowski K. Kinetics of Plasma Cell-Free DNA under a Highly Standardized and Controlled Stress Induction. *Cells* 2023; 12(4).
7. Hummel EM, Hessas E, Muller S, Beiter T, Fisch M, Eibl A, Wolf OT, Giebel B, Platen P, Kumsta R, Moser DA. Cell-free DNA release under psychosocial and physical stress conditions. *Transl Psychiatry* 2018; 8(1): 236.

8. Limberg AS, Berg F, Koper E, Lindgraf C, Gevers C, Kumsta R, Hummel EM, Moser DA. Cell-free DNA release following psychosocial and physical stress in women and men. *Transl Psychiatry* 2025; 15(1): 26.
9. Hu R, Li S, Stackpole ML, Li Q, Zhou XJ, Li W. cfTools: an R/Bioconductor package for deconvolving cell-free DNA via methylation analysis. *Bioinform Adv* 2025; 5(1): vbaf108.
10. Lehmann-Werman R, Neiman D, Zemmour H, Moss J, Magenheim J, Vaknin-Dembinsky A, Rubertsson S, Nellgard B, Blennow K, Zetterberg H, Spalding K, Haller MJ, Wasserfall CH, Schatz DA, Greenbaum CJ, Dorrell C, Grompe M, Zick A, Hubert A, Maoz M, Fendrich V, Bartsch DK, Golan T, Ben Sasson SA, Zamir G, Razin A, Cedar H, Shapiro AM, Glaser B, Shemer R, Dor Y. Identification of tissue-specific cell death using methylation patterns of circulating DNA. *Proc Natl Acad Sci U S A* 2016; 113(13): E1826–1834.
11. Lo YMD, Han DSC, Jiang P, Chiu RWK. Epigenetics, fragmentomics, and topology of cell-free DNA in liquid biopsies. *Science* 2021; 372(6538).
12. Loyfer N, Magenheim J, Peretz A, Cann G, Bredno J, Klochendler A, Fox-Fisher I, Shabi-Porat S, Hecht M, Pelet T, Moss J, Drawshy Z, Amini H, Moradi P, Nagaraju S, Bauman D, Shveiky D, Porat S, Dior U, Rivkin G, Or O, Hirshoren N, Carmon E, Pikarsky A, Khalaileh A, Zamir G, Grinbaum R, Abu Gazala M, Mizrahi I, Shussman N, Korach A, Wald O, Izhar U, Erez E, Yutkin V, Samet Y, Rotnemer Golinkin D, Spalding KL, Druid H, Arner P, Shapiro AMJ, Grompe M, Aravanis A, Venn O, Jamshidi A, Shemer R, Dor Y, Glaser B, Kaplan T. A DNA methylation atlas of normal human cell types. *Nature* 2023; 613(7943): 355–364.
13. Mattox AK, Douville C, Wang Y, Popoli M, Ptak J, Silliman N, Dobbyn L, Schaefer J, Lu S, Pearlman AH, Cohen JD, Tie J, Gibbs P, Lahouel K, Bettegowda C, Hruban RH, Tomasetti C, Jiang P, Chan KCA, Lo YMD, Papadopoulos N, Kinzler KW, Vogelstein B. The Origin of Highly Elevated Cell-Free DNA in Healthy Individuals and Patients with Pancreatic, Colorectal, Lung, or Ovarian Cancer. *Cancer Discov* 2023; 13(10): 2166–2179.
14. Moss J, Magenheim J, Neiman D, Zemmour H, Loyfer N, Korach A, Samet Y, Maoz M, Druid H, Arner P, Fu KY, Kiss E, Spalding KL, Landesberg G, Zick A, Grinshpun A, Shapiro AMJ, Grompe M, Wittenberg AD, Glaser B, Shemer R, Kaplan T, Dor Y. Comprehensive human cell-type methylation atlas reveals origins of circulating cell-free DNA in health and disease. *Nat Commun* 2018; 9(1): 5068.
15. Sadeh R, Sharkia I, Fialkoff G, Rahat A, Gutin J, Chappleboim A, Nitzan M, Fox-Fisher I, Neiman D, Meler G, Kamari Z, Yaish D, Peretz T, Hubert A, Cohen JE, Salah A, Temper M, Grinshpun A, Maoz M, Abu-Gazala S, Ben Ya'acov A, Shteyer E, Safadi R, Kaplan T, Shemer R, Planer D, Galun E, Glaser B, Zick A, Dor Y, Friedman N. ChIP-seq of plasma cell-free nucleosomes identifies gene expression programs of the cells of origin. *Nature Biotechnology* 2021; 39(5): 586–598.
16. Snyder MW, Kircher M, Hill AJ, Daza RM, Shendure J. Cell-free DNA Comprises an In Vivo Nucleosome Footprint that Informs Its Tissues-Of-Origin. *Cell* 2016; 164(1-2): 57–68.

17. Stanley KE, Jatsenko T, Tuveri S, Sudhakaran D, Lannoo L, Van Calsteren K, de Borre M, Van Parijs I, Van Coillie L, Van Den Bogaert K, De Almeida Toledo R, Lenaerts L, Tejpar S, Punie K, Rengifo LY, Vandenberghe P, Thienpont B, Vermeesch JR. Cell type signatures in cell-free DNA fragmentation profiles reveal disease biology. *Nature Communications* 2024; 15(1): 2220.
18. Sun K, Jiang P, Chan KC, Wong J, Cheng YK, Liang RH, Chan WK, Ma ES, Chan SL, Cheng SH, Chan RW, Tong YK, Ng SS, Wong RS, Hui DS, Leung TN, Leung TY, Lai PB, Chiu RW, Lo YM. Plasma DNA tissue mapping by genome-wide methylation sequencing for noninvasive prenatal, cancer, and transplantation assessments. *Proc Natl Acad Sci U S A* 2015; 112(40): E5503–5512.
19. Fridlich O, Peretz A, Fox-Fisher I, Pyanzin S, Dadon Z, Shcolnik E, Sadeh R, Fialkoff G, Sharkia I, Moss J, Arpinati L, Nice S, Nogiec CD, Ahuno ST, Li R, Taborda E, Dunkelbarger S, Fridlender ZG, Polak P, Kaplan T, Friedman N, Glaser B, Shemer R, Constantini N, Dor Y. Elevated cfDNA after exercise is derived primarily from mature polymorphonuclear neutrophils, with a minor contribution of cardiomyocytes. *Cell Rep Med* 2023; 4(6): 101074.
20. Nogiec CD, Karlic R, Taborda E, Dunkelbarger S, Fridlich O, Dor Y, Polak P, Li R. Exercise-Induced Cell-Free DNA Correlates with Energy Expenditure in Multiple Exercise Protocols. *Med Sci Sports Exerc* 2024; 56(5): 813–821.
21. Rodrigues KB, Weng Z, Graham ZA, Lavin K, McAdam J, Tuggle SC, Peoples B, Seay R, Yang S, Bamman MM, Broderick TJ, Montgomery SB. Exercise intensity and training alter the innate immune cell type and chromosomal origins of circulating cell-free DNA in humans. *Proc Natl Acad Sci U S A* 2025; 122(3): e2406954122.
22. Kirschbaum C, Pirke KM, Hellhammer DH. The 'Trier Social Stress Test'--a tool for investigating psychobiological stress responses in a laboratory setting. *Neuropsychobiology* 1993; 28(1-2): 76–81.
23. Simpson RJ, Kunz H, Agha N, Graff R. Exercise and the Regulation of Immune Functions. *Prog Mol Biol Transl Sci* 2015; 135: 355–380.
24. Fanninger S, Plener PL, Fischer MJ, Kothgassner OD, Goreis A. Water temperature during the cold pressor test: A scoping review. *Physiology & Behavior* 2023; 271: 114354.
25. Hines Jr EA, Brown GE. The cold pressor test for measuring the reactibility of the blood pressure: data concerning 571 normal and hypertensive subjects. *American heart journal* 1936; 11(1): 1–9.
26. Victor RG, Leimbach WN, Jr., Seals DR, Wallin BG, Mark AL. Effects of the cold pressor test on muscle sympathetic nerve activity in humans. *Hypertension* 1987; 9(5): 429–436.
27. Beiter T, Fragasso A, Hudemann J, Niess AM, Simon P. Short-term treadmill running as a model for studying cell-free DNA kinetics in vivo. *Clin Chem* 2011; 57(4): 633–636.
28. Berg F, Koper E, Limberg AS, Mattonet K, Budeus B, Kumsta R, Hummel EM, Moser DA. Development and validation of a novel cell type estimation method for targeted bisulfite sequencing data. *Epigenomics* 2025; 17(6): 389–396.
29. Ehlert T, Simon P, Moser DA. Epigenetics in sports. *Sports Med* 2013; 43(2): 93–110.

30. Davies RC, Rowlands AV, Eston RG. The prediction of maximal oxygen uptake from submaximal ratings of perceived exertion elicited during the multistage fitness test. *Br J Sports Med* 2008; 42(12): 1006–1010.
31. Moser DA, Braga L, Raso A, Zacchigna S, Giacca M, Simon P. Transgene detection by digital droplet PCR. *PLoS One* 2014; 9(11): e111781.
32. Krueger F, Andrews SR. Bismark: a flexible aligner and methylation caller for Bisulfite-Seq applications. *Bioinformatics* 2011; 27(11): 1571–1572.
33. Li H, Handsaker B, Wysoker A, Fennell T, Ruan J, Homer N, Marth G, Abecasis G, Durbin R, Genome Project Data Processing S. The Sequence Alignment/Map format and SAMtools. *Bioinformatics* 2009; 25(16): 2078–2079.
34. Gel B, Díez-Villanueva A, Serra E, Buschbeck M, Peinado MA, Malinverni R. regioneR: an R/Bioconductor package for the association analysis of genomic regions based on permutation tests. *Bioinformatics* 2016; 32(2): 289–291.
35. Posit team. RStudio: Integrated Development Environment for R. Posit Software, PBC: Boston, MA, 2026.
36. R Core Team. R: A Language and Environment for Statistical Computing. 4.5.1 edn. R Foundation for Statistical Computing: Vienna, Austria, 2026.
37. Beiter T, Niess AM, Moser D. Transcriptional memory in skeletal muscle. Don't forget (to) exercise. *J Cell Physiol* 2020; 235(7-8): 5476–5489.
38. Hu Z, Chen H, Long Y, Li P, Gu Y. The main sources of circulating cell-free DNA: Apoptosis, necrosis and active secretion. *Crit Rev Oncol Hematol* 2021; 157: 103166.
39. Moser DA, Tertel T, Berg F, Hummel EM, Platen P, Giebel B, Kumsta R. Stress type-specific small extracellular vesicle signatures reflect divergent biological responses to acute psychosocial and physical challenges *Sci Rep* 2025; 15(1): 35231.
40. Ince LM, Weber J, Scheiermann C. Control of Leukocyte Trafficking by Stress-Associated Hormones. *Front Immunol* 2018; 9: 3143.
41. Beiter T, Fragasso A, Hartl D, Niess AM. Neutrophil extracellular traps: a walk on the wild side of exercise immunology. *Sports Med* 2015; 45(5): 625–640.
42. Brinkmann V, Reichard U, Goosmann C, Fauler B, Uhlemann Y, Weiss DS, Weinrauch Y, Zychlinsky A. Neutrophil extracellular traps kill bacteria. *Science* 2004; 303(5663): 1532–1535.
43. Wang H, Kim SJ, Lei Y, Wang S, Wang H, Huang H, Zhang H, Tsung A. Neutrophil extracellular traps in homeostasis and disease. *Signal Transduct Target Ther* 2024; 9(1): 235.
44. Beltz NM, Gibson AL, Janot JM, Kravitz L, Mermier CM, Dalleck LC. Graded Exercise Testing Protocols for the Determination of VO(2)max: Historical Perspectives, Progress, and Future Considerations. *J Sports Med (Hindawi Publ Corp)* 2016; 2016: 3968393.
45. Gleeson M, Bishop NC, Stensel DJ, Lindley MR, Mastana SS, Nimmo MA. The anti-inflammatory effects of exercise: mechanisms and implications for the prevention and treatment of disease. *Nat*

Rev Immunol 2011; 11(9): 607–615.

46. Peake JM, Neubauer O, Walsh NP, Simpson RJ. Recovery of the immune system after exercise. *J Appl Physiol (1985)* 2017; 122(5): 1077–1087.

Figures

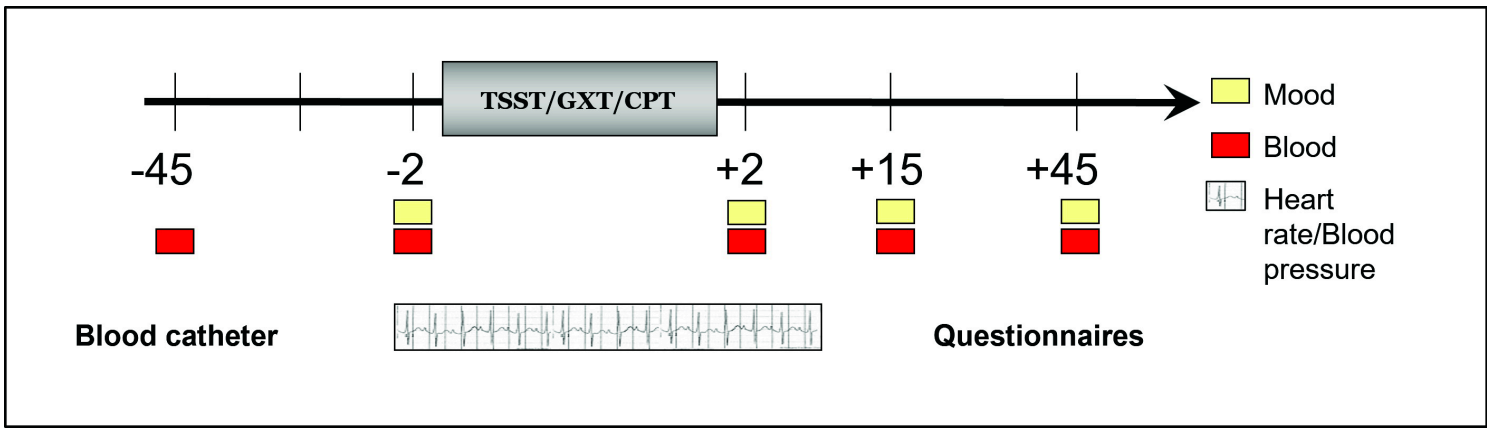


Figure 1

Study protocol

At −45 min, an indwelling blood catheter was inserted. Blood samples and mood ratings were obtained concurrently at −2, +2, +15 and +45 min relative to the experimental stressor (TSST, GXT, or CPT). Heart rate and blood pressure were monitored continuously throughout the protocol.

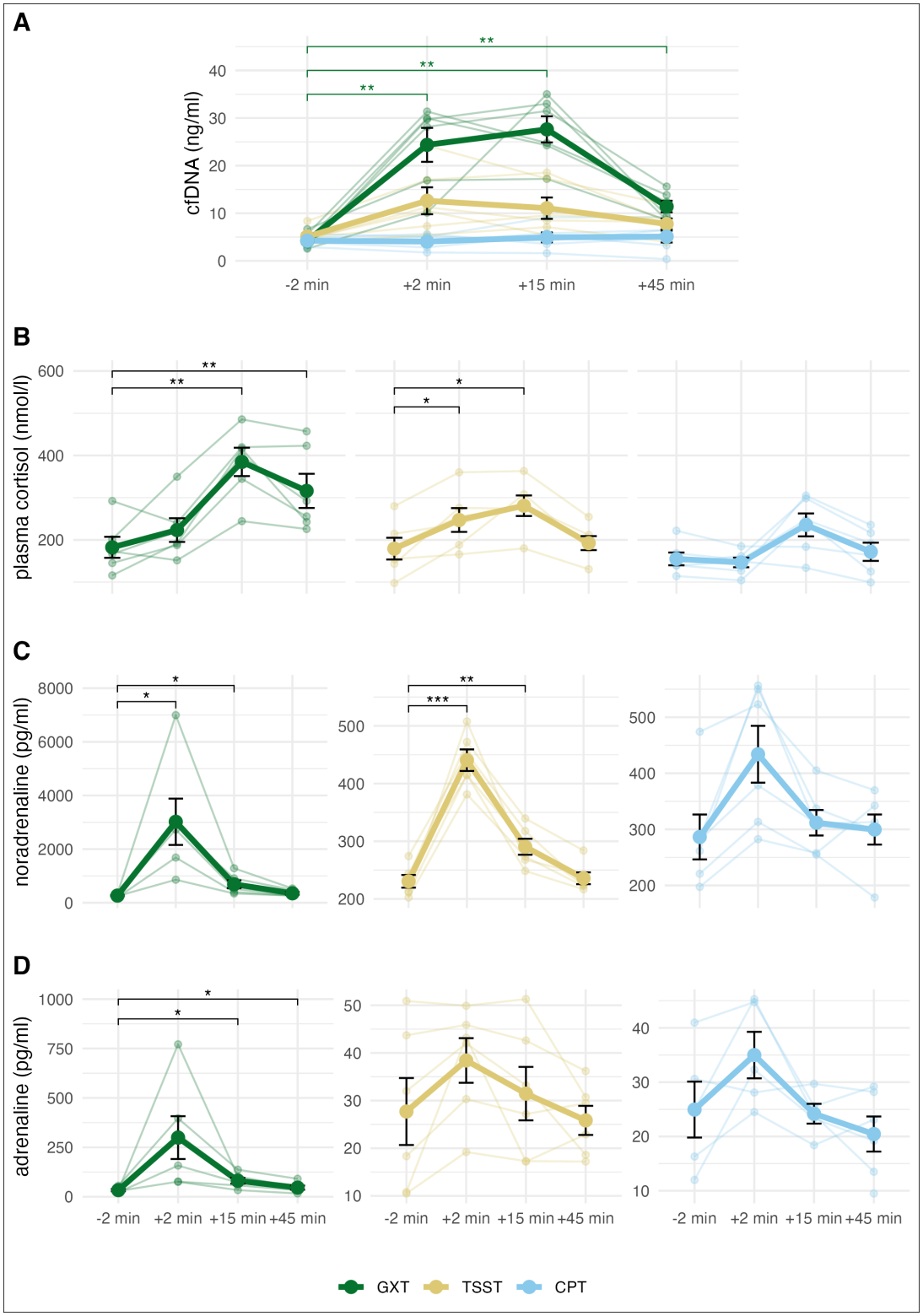


Figure 2

Stressor-specific changes in cfDNA and neuroendocrine markers

● GXT graded exercise test |● TSST psychosocial stress |● CPT cold pressor test

Plasma cfDNA (A), cortisol (B), noradrenaline (C), and adrenaline (D) were measured before and at +2, +15, and +45 min after the graded exercise test (GXT, green), Trier Social Stress Test (TSST, yellow), and Cold Pressor Test (CPT, blue). Thin colored lines and small markers indicate individual participants; bold lines and large markers show group means ± SEM. Asterisks indicate significant changes from baseline within each stress paradigm (p < .05, p < .01, p < .001).

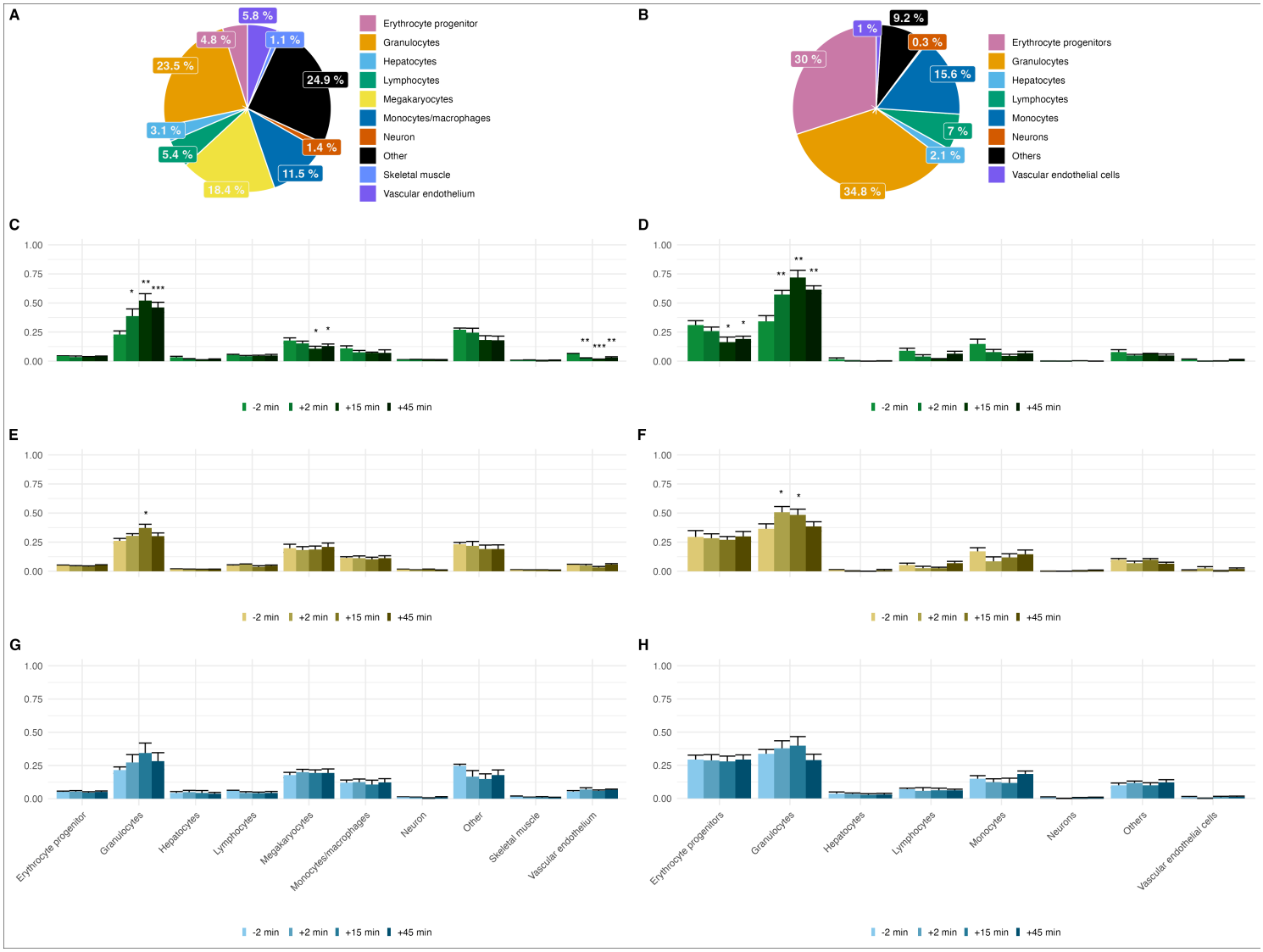


Figure 3

Cellular origin of cfDNA across acute stress paradigms

● GXT graded exercise test |● TSST psychosocial stress |● CPT cold pressor test

Pie charts show the overall cfDNA cell-type composition estimated using two complementary methylation-based deconvolution approaches (A, B). Plots on the left display cell types estimated with the UXM framework, while plots on the right show NNLS estimations. Temporal changes in cell-type contributions are shown for GXT (C, D), TSST (E, F), and CPT (G, H) at −2, +2, +15, and +45 min. Pie-chart colors indicate cell types according to the keys in panels A and B. Green, yellow, and blue bar shades indicate GXT, TSST, and

CPT, respectively; shade variants within each paradigm distinguish the four sampling time points. Bars represent group means ± SEM. Asterisks indicate significant changes from baseline within each stress paradigm (p < .05, p < .01, p <0.001).

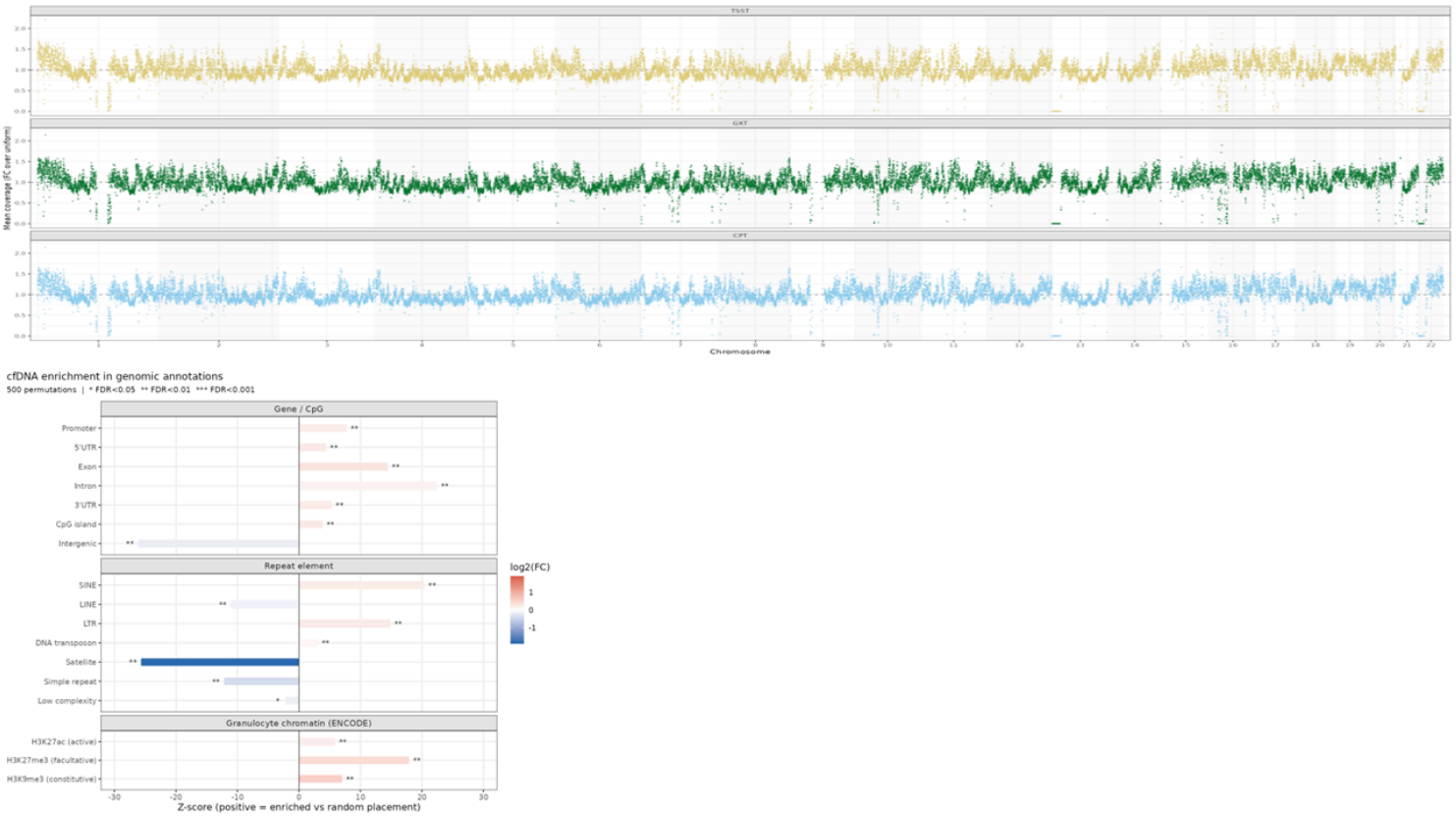


Figure 4

Genomic distribution and annotation enrichment of cfDNA

● GXT graded exercise test |● TSST psychosocial stress |● CPT cold pressor test

A) Genome-wide cfDNA coverage across chromosomes 1–22 following TSST, GXT, and CPT. Mean coverage relative to uniform genomic representation reveals highly similar, non-random regional patterns across all three stress paradigms.
*B) Enrichment of cfDNA fragments in genomic annotations assessed by regioneR permutation testing (500 permutations). Positive Z-scores indicate enrichment and negative scores depletion relative to random genomic placement; colour represents log_2 fold change. cfDNA was enriched in genic/CpG regions, SINE/LTR elements, and granulocyte chromatin states, whereas intergenic, satellite, LINE, and simple-repeat regions were depleted. *p < .05, **p < .01, ***p < .001*

Supplementary Files

This is a list of supplementary files associated with this preprint. Click to download.

- SupplementaryTable1.docx
- SupplementaryTable2.docx